

Divide, Evaluate, and Refine: Evaluating and Improving Text-to-Image Alignment with Iterative VQA Feedback

Jaskirat Singh¹

¹The Australian National University

Liang Zheng^{1,2}

²Australian Centre for Robotic Vision

<https://1jsingh.github.io/divide-evaluate-and-refine>



Figure 1: We propose a training-free decompositional framework which helps both better evaluate (Sec. 3.1) and gradually improve (Sec. 3.2) text-to-image alignment using iterative VQA feedback.

Abstract

The field of text-conditioned image generation has made unparalleled progress with the recent advent of latent diffusion models. While remarkable, as the complexity of given text input increases, the state-of-the-art diffusion models may still fail in generating images which accurately convey the semantics of the given prompt. Furthermore, it has been observed that such misalignments are often left undetected by pretrained multi-modal models such as *CLIP*. To address these problems, in this paper we explore a simple yet effective decompositional approach towards both evaluation and improvement of text-to-image alignment. In particular, we first introduce a *Decompositional-Alignment-Score* which given a complex prompt decomposes it into a set of disjoint assertions. The alignment of each assertion with generated images is then measured using a VQA model. Finally, alignment scores for different assertions are combined a posteriori to give the final text-to-image alignment score. Experimental analysis reveals that the proposed alignment metric shows significantly higher correlation with human ratings as opposed to traditional *CLIP*, *BLIP* scores. Furthermore, we also find that the assertion level alignment scores provide a useful feedback which can then be used in a simple iterative procedure to gradually increase the expression of different assertions in the final image outputs. Human user studies indicate that the proposed approach surpasses previous state-of-the-art by 8.7% in overall text-to-image alignment accuracy.



Figure 2: *Overview.* *Top:* Traditional methods for evaluating text-to-image alignment *e.g.*, CLIP [9], BLIP-2 [10] and BLIP2-ITM (which provides a binary image-text matching score between 0 and 1) often fail to distinguish between good (*right*) and bad (*left*) image outputs and can give high scores even if the generated image is not an accurate match for input prompt (missing yellow car). In contrast, by breaking down the prompt into a set of disjoint assertions and then evaluating their alignment with the generated image using a VQA model [10], the proposed Compositional-Alignment Score (DA-score) shows much better correlation with human ratings (refer Sec. 4.1). *Bottom:* Furthermore, we show that the assertion-level alignment scores can be used along with a simple iterative refinement strategy to reliably improve the alignment of generated image outputs (refer Sec. 4.2).

1 Introduction

The field of text-to-image generation has made significant advancements with the recent advent of large-scale language-image (LLI) models [1–5]. In particular, text-conditioned latent diffusion models have shown unparalleled success in generating creative imagery corresponding to a diverse range of free-form textual descriptions. However, while remarkable, it has been observed [6–8] that as the complexity of the input text increases, the generated images do not always accurately align with the semantic meaning of the textual prompt.

To facilitate the reliable use of current text-to-image generation models for practical applications, it is essential to answer two key questions: 1) Can we detect such fine-grain misalignments between the input text and the generated output in a robust manner? and 2) Once detected, can we improve the text-to-image alignment for failure cases? While several metrics for evaluating text-to-image alignment (*e.g.*, CLIP [9], BLIP [10], BLIP2 [11]) exist, it has been observed [7, 12] that a high score with these metrics can be achieved even if the image does not fully correspond with input prompt. For instance, in Fig. 2, an output image (containing only pink trees) shows high CLIP/BLIP scores with the text “pink trees and yellow car” even if yellow car is not present. Evaluating text-to-image matching using the image-text-matching (ITM) head of BLIP models has also been recently explored [10, 11]. However, the generated scores also show a similar tendency to favor the main subject of input prompt. Furthermore, even if such misalignments are detected, it is not clear how such information can be used for improving the quality of generated image outputs in a reliable manner.

To address these problems, in this paper we explore a simple yet effective compositional approach towards both evaluation and improvement of fine-grain text-to-image alignment. In particular, we propose a *Compositional-Alignment-Score* (DA-Score) which given a complex text prompt, first decomposes it into a set of disjoint assertions about the content of the prompt. The alignment of each of these assertions with the generated image is then measured using a VQA model [10, 13]. Finally, the alignment scores for different assertions are combined to give an overall text-to-image

a couple wearing scuba gear having a tea party underwater with a school of fish



a man riding a skateboard down a mountain road while holding an umbrella and wearing goggles.



Figure 3: *Iterative refinement (Col:1-3;4-6) for improving text-to-image alignment.* We propose a simple iterative refinement approach which uses the decompositional alignment scores (refer Sec. 3.1) as feedback to gradually improve the alignment of the generated images with the input text-prompt.

alignment score. Our experiments reveal that the proposed evaluation score shows significantly higher correlation with human ratings over prior evaluation metrics (*e.g.*, CLIP, BLIP, BLIP2) (Sec. 4.1).

Furthermore, we also find that the assertion-level alignment scores provide a useful and explainable feedback for determining which parts of the input prompt are not being accurately described in the output image. We show that this feedback can then be used to gradually improve the alignment of the generated images with the input text prompt. To this end, we propose a simple iterative refinement procedure (Fig. 3), wherein at each iteration the expressivity of the least-aligned assertion is improved by increasing the weightage/cross-attention strength (refer Sec. 3.2) of corresponding prompt tokens during the reverse diffusion process. Through both qualitative and quantitative analysis, we find that the proposed iterative refinement process allows for generation of better aligned image outputs over prior works [6–8] while on average showing comparable inference times (Sec. 4.2).

2 Related Work

Text to Image Generation Models. Text conditional image synthesis is a topic of keen interest in the vision community. For instance, [14–18] use GANs to perform text guided image generation. Similarly, [5, 19] explore the use of autoregressive models for zero-shot text to image generation. Recently, diffusion-based-models [1–5, 20, 21] have emerged as a powerful class of methods for performing text-conditional image synthesis over diverse range of target domains.

While remarkable, generating images which align perfectly with the input text-prompt remains a challenging problem [6–8, 22]. To enforce, heavier reliance of generated outputs on the provided text, classifier-free guidance methods [2, 3, 23] have been proposed. Similarly, use of an additional guidance input to improve controllability of text-to-image generation have recently been extensively explored [24–35]. However, even with their application, the generated images are often observed to exhibit fine-grain misalignments such as missing secondary objects [6, 7] with the input text prompt.

Evaluating Image-Text Alignment. Various protocols for evaluating text-image alignment in a reference-free manner have been proposed [9–11]. Most prior works [2, 3, 5, 9] typically use the cosine similarity between the text and image embedding from large-scale multi-modal models [9, 36–38] such as CLIP [9], BLIP [10], BLIP-2 [11] for evaluating the alignment scores. Recently, [10, 11] also show the application of BLIP/BLIP-2 models for image-text matching using image retrieval. However, as shown in Fig. 2, these scores can give very high scores even if the generated images do not full align with the input text prompt. Furthermore, unlike our approach image-text alignment is often represented through a single scalar value which does not provide an explainable measure which can be used to identify/improve weaknesses of the image generation process.

Recent contemporary work [39] also explores the idea of VQA for evaluating T2I alignment. However, the use of VQA is limited to evaluation alone. In contrast, we further demonstrate how the interpretability of VQA scores can then be used to reliably improve the performance of T2I models.

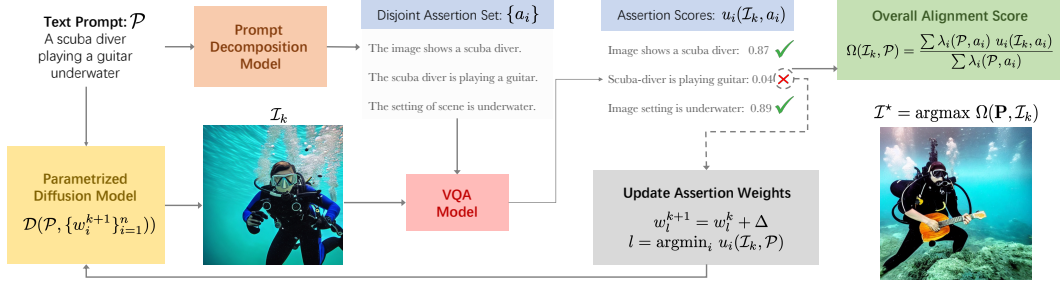


Figure 4: *Method Overview*. Given a text prompt \mathcal{P} and an initially generated output \mathcal{I}_0 , we first generate a set of disjoint assertions a_i regarding the content of the caption. The alignment of the output image \mathcal{I}_0 with each of these assertions is then calculated using a VQA model. Finally, we use the assertion-based-alignment scores $u_i(\mathcal{I}_0, \mathcal{P})$ as feedback to increase the weightage w_i (of the assertion with least alignment score) in a parameterized diffusion model formulation \mathcal{D} (Sec. 3.2). This process can then be performed in an iterative manner to gradually improve the quality of the generated outputs until a desirable threshold for the overall alignment score $\Omega(\mathcal{I}_k, \mathcal{P})$ is reached.

Improving Image-Text Alignment. Recently several works [6–8] have been proposed to explore the problem of improving image-text alignment in a training free manner. Liu *et al.* [6] propose to modify the reverse diffusion process by composing denoising vectors for different image components. However, it has been observed [7] that it struggles while generating photorealistic compositions of diverse objects. Feng *et al.* [8] use scene graphs to split the input sentence into several noun phrases and then assign a designed attention map to the output of the cross-attention operation. In another recent work, Chefer *et al.* [7] extend the idea of cross-attention map modification to minimize missing objects but instead do so by modifying the noise latents during the reverse diffusion process. While effective at reducing missing objects, we find that the performance / quality of output images can suffer as the number of subjects in the input prompt increases (refer Sec. 4.2).

Besides training-free methods, recent contemporary work [40, 41] has also explored the possibility of improving image-text alignment using human feedback to finetune existing latent diffusion models. However this often requires the collection of large-scale human evaluation scores and finetuning the diffusion model across a range of diverse data modalities which can be expensive. In contrast, we explore a training free approach for improvement of fine-grain text-to-image alignment.

3 Our Method

Given the image generation output \mathcal{I} corresponding to a text prompt \mathcal{P} , we wish to develop a mechanism for evaluation and improvement of fine-grain text-to-image alignment. The core idea of our approach is to take a decompositional strategy for both these tasks. To this end, we first generate a set of disjoint assertions regarding the content of the input prompt. The alignment of the output image \mathcal{I} with each of these assertions is then calculated using a VQA model. Finally, we use the assertion-based-alignment scores as feedback to improve the expressiveness of the assertion with the least alignment score. This process can then be performed in an iterative manner to gradually improve the quality of generated outputs until a desired value for the overall alignment score is attained.

In the next sections, we discuss each of these steps in detail. In Sec. 3.1 we first discuss the process for evaluating decompositional-alignment scores. We then discuss the iterative refinement process for improving text-to-image alignment in Sec. 3.2. Fig. 4 provides an overview for the overall approach.

3.1 Evaluating Text-to-Image Alignment

Prompt Decomposition Model. Given an input prompt \mathcal{P} , we first decompose its textual information into a set of disjoint assertions (and corresponding questions) which exhaustively cover the contents of the input prompt. Instead of relying on human-inputs as in [6, 7]¹, we leverage the in-context

¹Prior works on improving image-text alignment often rely on human-user inputs for expressing contents of the input prompt into its simpler constituents. For instance, Feng *et al.* [6] require the user to describe the prompt as a conjunction/disjunction of simpler statements. Similarly, Chefer *et al.* [7] require the user to provide a set of entities / subjects in the prompt, over which their optimization should be performed.




	Prompt \mathcal{P} : A scuba diver <i>playing a guitar</i> underwater		
	Sub-prompts: $\{p_i\}$	Disjoint Assertion Set: $\{a_i\}$	Question Rephrasing: $\{a_i^q\}$
	a scuba diver. <i>playing a guitar</i> underwater	The image shows a scuba diver. The scuba diver is playing a guitar. The setting of scene is underwater.	Does the image show a scuba diver? Is scuba diver playing a guitar? Is setting of scene underwater?
	Prompt \mathcal{P} : A horse on a beach <i>wearing sunglasses</i>		
	Sub-prompts: $\{p_i\}$	Disjoint Assertion Set: $\{a_i\}$	Question Rephrasing: $\{a_i^q\}$
	a horse on a beach <i>wearing sunglasses</i>	The image shows a horse. The horse is on a beach. The horse is wearing sunglasses.	Does the image show a horse? Is the horse on a beach? Is the horse wearing sunglasses?
	Prompt \mathcal{P} : A dolphin <i>wearing a party hat</i> at a pool party		
	Sub-prompts: $\{p_i\}$	Disjoint Assertion Set: $\{a_i\}$	Question Rephrasing: $\{a_i^q\}$
	a dolphin <i>wearing a party hat</i> at a pool party	The image shows a dolphin. The dolphin is wearing a party hat. The setting of image is a pool party.	Does the image show a dolphin? Is dolphin wearing a party hat? Is setting of image pool party?

Figure 5: Visualizing the prompt decomposition process. By dividing a complex prompt \mathcal{P} into a set of disjoint assertions a_i , we are able to identify the sub-prompts p_i (circled) which are not expressed in the image output using VQA, and thereby address them using iterative refinement (Sec. 3.2).

learning capability [42] of large-language models [43, 44] for predicting such decompositions in an autonomous manner. In particular, given an input prompt \mathcal{P} and large-language model \mathcal{M} , the prompt decomposition is performed using in-context learning as,

$$\mathbf{x} = \{x_0, x_1, \dots, x_n\} = \mathcal{M}(\mathbf{x} \mid \mathcal{P}, D_{\text{exemplar}}, \mathcal{T}), \quad (1)$$

where \mathbf{x} is the model output, n is the number of decompositions, D_{exemplar} is the in-context learning dataset consisting 4-5 human generated examples for prompt decomposition, and \mathcal{T} is task description. Please refer supp. material for further details on exemplar-dataset and task-description design.

The model output \mathbf{x} is predicted to contain tuples $x_i = \{a_i, p_i\}$, where each tuple is formatted to contain assertions a_i and the sub-part p_i of the original prompt \mathcal{P} corresponding to the generated assertion. For instance, given \mathcal{P} : ‘a cat and a dog’ the prompt decomposition can be written as,

$$\mathcal{M}(\mathbf{x} \mid \mathcal{P} : \text{‘a cat and a dog’}, D_{\text{exemplar}}, \mathcal{T}) = [\{\text{‘there is a cat’}, \text{‘a cat’}\}, \{\text{‘there is a dog’}, \text{‘a dog’}\}].$$

Computing Assertion-based Alignment Scores. We next compute the alignment of the generated image \mathcal{I} with each of the disjoint assertions using a Visual-Question-Answering (VQA) model [10]. In particular, given image \mathcal{I} , assertions $a_i, i = 1, \dots, n$, their rephrasing in question format a_i^q and VQA-model \mathcal{V} , the assertion-level alignment scores $u_i(\mathcal{I}, a_i)$ are computed as,

$$u_i(\mathcal{I}, a_i) = \frac{\exp(\alpha_i/\tau)}{\exp(\alpha_i/\tau) + \exp(\beta_i/\tau)}, \text{ where } \alpha_i = \mathcal{V}(\text{‘yes’} \mid \mathcal{I}, a_i^q), \quad \beta_i = \mathcal{V}(\text{‘no’} \mid \mathcal{I}, a_i^q),$$

where α_i, β_i refer to the logit-scores of VQA-model \mathcal{V} for input tuple (image \mathcal{I} , question a_i^q) corresponding to output tokens ‘yes’, ‘no’ respectively. Hyperparameter τ controls the temperature of the softmax operation and controls the confidence of the alignment predictions.

Combining Alignment Scores. Finally, the assertion level alignment-scores $u_i(\mathcal{I}, a_i)$ are combined to give the overall text-to-image alignment score $\Omega(\mathcal{I}, \mathcal{P})$ between image \mathcal{I} and prompt \mathcal{P} as,

$$\Omega(\mathcal{I}, \mathcal{P}) = \frac{\sum_i \lambda_i(\mathcal{P}, a_i) u_i(\mathcal{I}, a_i)}{\sum_i \lambda_i(\mathcal{P}, a_i)}, \quad (2)$$

where weights $\lambda_i(\mathcal{P}, a_i)$ refer to the importance of assertion a_i in capturing the overall content of the input prompt \mathcal{P} , and allows the user to control the relative importance of different assertions in generating the final image output². Please refer Fig. 4 for the overall implementation.

²For simplicity reasons, we mainly use $\lambda_i = 1 \forall i$ in the main paper. Further analysis on variable λ_i to account for variable information content or visual verifiability of an assertion are provided in supp. material.

3.2 Improving Text to Image Alignment

In addition to predicting overall text-to-image alignment score, we find that assertion-level alignment scores $u_i(\mathcal{I}, a_i)$ also provide a useful and explainable way for determining which parts of the input prompt \mathcal{P} are not being accurately described in the output image \mathcal{I} . This feedback can then be used in an iterative manner to improve the expressivity of the assertion with least alignment score $u_i(\mathcal{I}, q_i)$, until a desired threshold for the overall text-image alignment score $\Omega(\mathcal{I}, \mathcal{P})$ is obtained.

Parameterized Diffusion Model. We first modify the image generation process of standard diffusion models in order to control the expressiveness of different assertions a_i in parametric manner. In particular, we modify the reverse diffusion process to also receive inputs weights w_i , where each w_i controls the relative importance of assertion a_i during the image generation process. In this paper, we mainly consider the following two methods for obtaining such parametric control.

Prompt Weighting. Instead of computing the CLIP [36] features from original prompt \mathcal{P} we use prompt-weighting [45] to modify the input CLIP embeddings to the diffusion model as,

$$\text{CLIP}(\mathcal{P}) = \mathcal{W}(\mathcal{P}, \{\text{CLIP}(p_i), w_i\}_{i=1}^n) \quad (3)$$

where \mathcal{W} refers to the prompt-weighting function from [1, 45], p_i refers to the sub-prompt (Sec. 3.1) corresponding to assertion a_i , and weights w_i control the relative weight of different sub-prompts p_i in computing the overall CLIP embedding for prompt \mathcal{P} .

Cross-Attention Control. Similar to [7], we also explore the idea of modifying the noise latents z_t during the reverse diffusion process, to increase the cross-attention strength of the main noun-subject for each sub-assertion a_i . However, instead of only applying the gradient update for the least dominant subject [7], we modify the loss for the latent update in parametric form as,

$$z_t = z_t - \alpha \nabla_{z_t} \mathcal{L}(z_t, \{w_i\}_{i=1}^n), \text{ where } \mathcal{L}(z_t, \{w_i\}_{i=1}^n) = \sum_i w_i (1 - \max G(\mathcal{A}_i^t)), \quad (4)$$

where α is the step-size, \mathcal{A}_i^t refer to the attention map corresponding to the main noun-subject in assertion a_i , G is a smoothing function and weights w_i control the extent to which the expression of different noun-subjects in the prompt (for each assertion) will be increased in the next iteration.

Iterative Refinement. Given the above parametric formulation for controlling expression of different assertions, we next propose a simple yet effective iterative refinement approach towards improving text-to-image alignment. In particular, at any iteration $k \in [1, 5]$ during the refinement process, we first compute both overall text-image similarity score $\Omega(\mathcal{I}_k, \mathcal{P})$ and assertion-level alignment scores $u_i(\mathcal{I}_k, \mathcal{P})$. The image generation output \mathcal{I}_{k+1} for the next iteration is then computed as,

$$\mathcal{I}_{k+1} = \mathcal{D}(\mathcal{P}, \{w_i^{k+1}\}_{i=1}^n); \text{ where } w_i^{k+1} = \begin{cases} w_i^k + \Delta, & \text{if } i = \text{argmin}_l u_l(\mathcal{I}, \mathcal{P}) \\ w_i^k & \text{otherwise} \end{cases}, \quad (5)$$

where \mathcal{D} refers to the parametrized diffusion model and Δ is a hyper-parameter. This iterative process is then performed until a desirable threshold for the overall alignment score $\Omega(\mathcal{I}_k, \mathcal{P})$ is reached. The image generation output \mathcal{I}^* at the end of the refinement process is then computed as,

$$\mathcal{I}^* = \text{argmax}_{\mathcal{I}_k} \Omega(\mathcal{I}_k, \mathcal{P}). \quad (6)$$

4 Experiments

Dataset. Since there are no openly available datasets addressing semantic challenges in text-based image generation with human annotations, we introduce a new benchmark dataset Decomposable-Captions-4k for method comparison. The dataset consists an overall of 24960 human annotations on images generated using all methods [1, 6, 7] (including ours) across a diverse set of 4160 input prompts. Each image is a given rating between 1 and 5 (where 1 represents that ‘image is irrelevant to the prompt’ and 5 represents that ‘image is an accurate match for the prompt’).

Furthermore, unlike prior works [7] which predominantly analyse the performance on relatively simple prompts with two subjects (e.g. object a and object b), we construct a systematically diverse pool of input prompts for better understanding text-to-image alignment across varying complexities in the text prompt. In particular, the prompts for the dataset are designed to encapsulate two axis of

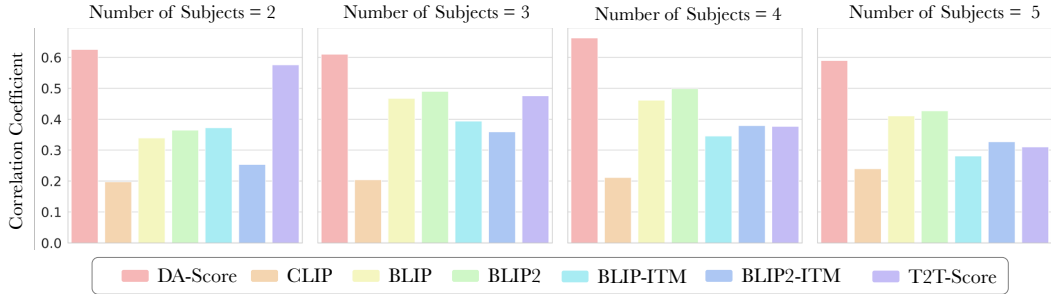


Figure 6: *Method comparisons w.r.t correlation with human ratings.* We compare the correlation of different text-to-image alignment scores with those obtained from human subjects, as the number of subjects in the input prompt (refer Sec. 4) is varied. We observe that the proposed alignment score (DA-score) provides a better match for human-ratings over traditional text-to-image alignment scores.

complexity: *number of subjects* and *realism*. The number of subjects refers to the number of main objects described in the input prompt and varies from 2 (e.g., *a cat with a ball*) to 5 (e.g., *a woman walking her dog on a leash by the beach during sunset*). Similarly, the *realism* of a prompt is defined as the degree to which different concepts naturally co-occur together and varies as *easy*, *medium*, *hard* and *very hard*. *easy* typically refers to prompts where concepts are naturally co-occurring together (e.g., *a dog in a park*) while *very hard* refers to prompts where concept combination is very rare (e.g., *a dog playing a piano*). Further details regarding the dataset are provided in supplementary material.

4.1 Evaluating Text-to-Image Alignment

Baselines. We compare the performance of the *Decompositional-Alignment Score* with prior works on evaluating text-to-image alignment in a reference-free manner. In particular, we show comparisons with CLIP [9], BLIP [10] and BLIP2 [11] scores where the text-to-image alignment score is computed using the cosine similarity between the corresponding image and text embeddings. We also include comparisons with BLIP-ITM and BLIP2-ITM which directly predict a binary image-text matching score (between 0 and 1) for input prompt and output image. Finally, we report results on the recently proposed text-to-text (T2T) similarity metric [7] which computes image-text similarity as the average cosine similarity between input prompt and captions generated (using BLIP) from the input image.

Quantitative Results. Fig. 6 shows the correlation between human annotations and predicted text-to-image alignment scores across different metrics on the *Decomposable-Captions* dataset. We observe that the *DA-Score* shows a significantly higher correlation with human evaluation ratings as opposed to prior works across varying number of subjects $N \in [2, 5]$ in the input prompt. We also note that while the recently proposed T2T similarity score [7] shows comparable correlation with ours for $N = 2$, its performance significantly drops as the number of subjects in the input prompt increases.

4.2 Improving Text-to-Image Alignment

In this section, we compare the performance of our iterative refinement approach with prior works on improving text-to-image alignment in a training-free manner. In particular, we show comparisons with 1) Stable Diffusion [1], 2) Composable Diffusion [6] 3) StructureDiffusion [8] and 4) Attend-and-Excite [7]. All images are generated using the same seed across all methods.

Qualitative Results. Results are shown in Fig. 7. As shown, we observe that Composable Diffusion [6] struggles to generate photorealistic combinations of objects especially as number of subjects in the prompt increase. StructureDiffusion [8] helps in addressing some missing objects e.g., telescope in example-1, but the generated images tend to be semantically similar to those produced by the original Stable Diffusion model, and thus does not significantly improve text-to-image alignment.

Attend-and-Excite [7] shows much better performance in addressing missing objects (e.g., telescope in example-1 and umbrella in example-4). However, as summarized in Fig. 8 we observe that it suffers from 3 main challenges: 1) *Object Relationship* (Fig. 8a): we observe that despite having desired objects, generated images may sometimes fail to convey relationship between them. For e.g., in row-1 Fig. 8 while output images show both a *lion and guitar*, the lion does not seem to be playing the guitar. In contrast, Eval-and-Refine is able to describe both presence and relation between

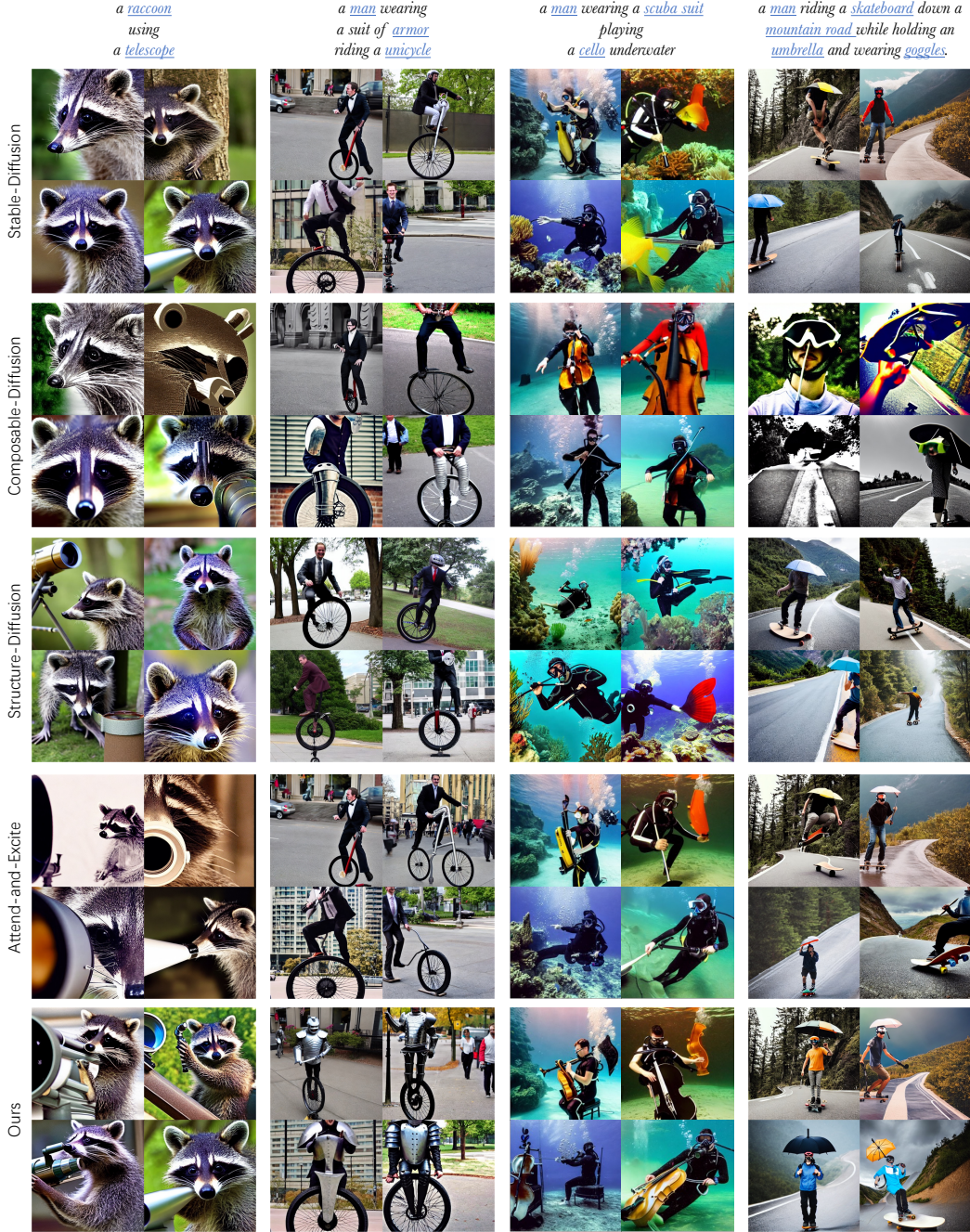


Figure 7: *Qualitative comparison w.r.t text-to-image alignment.* We compare the outputs of our iterative refinement approach with prior works [1, 6–8] on improving quality of generated images with changing number of subjects (underlined) from 2 to 5. Please zoom-in for best comparisons.

objects in a better manner. 2) *Overlapping Entities* (Fig. 8b): For images with overlapping entities (e.g., *person* and *spacesuit*), we observe that Attend-and-Excite [7] typically spends most of gradient updates balancing between the overlapping entities, as both entities (*person* and *spacesuit*) occupy the same cross-attention region. This can lead to outputs where a) other important aspects (e.g., *lake* in Col-3) or b) one of the two entities (e.g., *spacesuit*) are ignored. 3) *Prompt Complexity* (Fig. 8c): Finally, we note that since Attend-and-Excite [7] is limited to applying the cross-attention update w.r.t the least dominant subject, as the complexity of input prompt \mathcal{P} increases, it may miss some objects (e.g., *umbrella*, *beach*, *sunny day*) during the generation process. In contrast, the iterative

Prompt: A lion playing a guitar



(a) *Object Relationship*: Eval-and-Refine helps better capture both presence and relationship between the objects.

Prompt: A person in a spacesuit riding a bicycle by the lake



(b) *Overlapping entities*: Proposed approach can better handle cases with overlapping entities (spacesuit, person).

Prompt: a snowman wearing sunglasses holding an umbrella on a beach on a sunny day



(c) *Prompt Complexity*: Eval-and-Refine shows better alignment as number of subjects in input prompt increase.

Figure 8: *Additional comparisons with Attend-and-Excite*. We analyse three main ways in which the proposed iterative-refinement improves over Attend-and-Excite [7] (refer Sec. 4.2 for details).

nature of our approach allows it to keep refining the output image \mathcal{I} until a desirable threshold for the overall image-text alignment score $\Omega(\mathcal{I}, \mathcal{P})$ is reached.

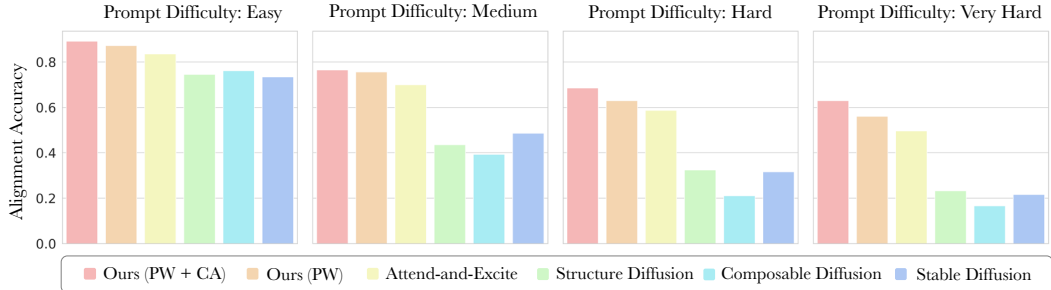


Figure 9: *Variation of alignment accuracy with prompt difficulty.* We observe that while the accuracy of all methods decreases with increasing difficulty in prompt *realism* (refer Sec. 4), the proposed iterative refinement approach consistently performs better than prior works.

Method	Norm. Human Score (%)	Alignment Accuracy (%)	Pairwise Comparison %			Inference Time (s)
			Win ↑	Tie	Lose ↓	
Stable-Diffusion [1]	72.98	43.66	41.7	50.1	8.2	3.54 s
Composable-Diffusion [6]	70.28	37.72	57.1	38.5	4.4	10.89 s
Structure-Diffusion [8]	74.93	45.23	37.5	54.6	7.9	11.51 s
Attend-and-Excite [7]	85.94	65.50	23.6	62.3	14.1	8.59 s
Ours (PW)	89.53	70.28	N/A	N/A	N/A	10.32 s
Ours (PW + CA)	90.25	74.16	N/A	N/A	N/A	12.24 s

Table 1: *Quantitative Results.* We report text-to-image alignment comparisons *w.r.t* normalized human rating score (Col:2), average alignment accuracy evaluated by human subjects (Col:3) and pairwise user-preference scores (ours vs prior work) (Col:4-6). Finally, we also report average inference time per image for different methods in Col:7. We observe that our approach shows better text-to-image alignment performance while on average using marginally higher inference time.

Quantitative Results. In addition to qualitative experiments, we also evaluate the efficacy of our approach using human evaluations. In this regard, we report three metrics: 1) *normalized human score*: which refers to the average human rating (normalized between 0-1) for images generated on the Decomposable-Captions-4k dataset. 2) *accuracy*: indicating the percentage of generated images which are considered as an accurate match (rating: 5) for the input text prompt by a human subject. 3) *pairwise-preference*: where human subjects are shown pair of images generated using our method and prior work, and are supposed to classify each image-pair as a win, loss or tie (win meaning our method is preferred). For our approach we consider two variants 1) *Ours (PW)* which performs iterative refinement using only prompt-weighting, and 2) *Ours (PW + CA)* where iterative refinement is performed using both prompt weighting and introducing cross-attention updates (Sec. 3.2). Pairwise preference scores are reported while using *Ours (PW + CA)* while comparing with prior works.

Results are shown in Fig. 9 and Tab. 1. We observe that while the text-to-image alignment accuracy for all methods decreases with an increased difficulty in input text prompts (Fig. 9), we find that the our approach with only prompt-weighting is able to consistently perform on-par or better than Attend-and-Excite [7]. Further introduction of cross-attention updates (Sec. 3.2), allows our approach to exhibit even better performance, which outperforms Attend-and-Excite [7] by 8.67 % in terms of overall alignment accuracy of the generated images. These improvements are also reflected in the pairwise comparisons where human subjects tend to prefer our approach over prior works [6–8].

Inference time comparison. Tab. 1 shows comparison for the average inference time (per image) for our approach with prior works [6–8]. We observe that despite the use of an iterative process for our approach, the overall inference time is comparable with prior works. This occurs because prior works themselves often include additional steps. For instance, Composable-Diffusion [6] requires the computation of separate denoising latents for each statement in the conjunction/disjunction operation, thereby increasing the overall inference time almost linearly with number of subjects. Similarly, Attend-and-Excite [7] includes additional gradient descent steps for modifying cross-attention maps. Moreover, such an increase is accumulated even if the baseline Stable-Diffusion [1] model already generates accurate images. In contrast, the proposed iterative refinement approach is able to adaptively

adjust the number of iterations required for the generation process by monitoring the proposed *DA-Score* for evaluating whether the generation outputs are already good enough.

5 Conclusion

In this paper, we explore a simple yet effective decompositional approach for both evaluation and improvement of text-to-image alignment with latent diffusion models. To this end, we first propose a *Decompositional-Alignment Score* which given a complex prompt breaks it down into a set of disjoint assertions. The alignment of each of these assertions with the generated image is then measured using a VQA model. The assertion-based alignment scores are finally combined to give an overall text-to-image alignment score. Experimental results show that proposed metric shows significantly higher correlation with human subject ratings over traditional CLIP, BLIP based image-text matching scores. Finally, we propose a simple iterative refinement approach which uses the decompositional-alignment scores as feedback to gradually improve the quality of the generated images. Despite its simplicity, we find that the proposed approach is able to surpass previous state-of-the-art on text-to-image alignment accuracy while on average using only marginally higher inference times. We hope that our research can open new avenues for robust deployment of text-to-image models for practical applications.

References

- [1] Robin Rombach, Andreas Blattmann, Dominik Lorenz, Patrick Esser, and Björn Ommer. High-resolution image synthesis with latent diffusion models, 2021. [2](#), [3](#), [6](#), [7](#), [8](#), [10](#), [18](#), [19](#), [20](#), [21](#), [27](#)
- [2] Alex Nichol, Prafulla Dhariwal, Aditya Ramesh, Pranav Shyam, Pamela Mishkin, Bob McGrew, Ilya Sutskever, and Mark Chen. Glide: Towards photorealistic image generation and editing with text-guided diffusion models. *arXiv preprint arXiv:2112.10741*, 2021. [3](#)
- [3] Chitwan Saharia, William Chan, Saurabh Saxena, Lala Li, Jay Whang, Emily Denton, Seyed Kamyar Seyed Ghasemipour, Burcu Karagol Ayan, S Sara Mahdavi, Rapha Gontijo Lopes, et al. Photorealistic text-to-image diffusion models with deep language understanding. *arXiv preprint arXiv:2205.11487*, 2022. [3](#)
- [4] Aditya Ramesh, Prafulla Dhariwal, Alex Nichol, Casey Chu, and Mark Chen. Hierarchical text-conditional image generation with clip latents. *arXiv preprint arXiv:2204.06125*, 2022.
- [5] Jiahui Yu, Yuanzhong Xu, Jing Yu Koh, Thang Luong, Gunjan Baid, Zirui Wang, Vijay Vasudevan, Alexander Ku, Yinfei Yang, Burcu Karagol Ayan, et al. Scaling autoregressive models for content-rich text-to-image generation. *arXiv preprint arXiv:2206.10789*, 2022. [2](#), [3](#)
- [6] Nan Liu, Shuang Li, Yilun Du, Antonio Torralba, and Joshua B Tenenbaum. Compositional visual generation with composable diffusion models. In *Computer Vision—ECCV 2022: 17th European Conference, Tel Aviv, Israel, October 23–27, 2022, Proceedings, Part XVII*, pages 423–439. Springer, 2022. [2](#), [3](#), [4](#), [6](#), [7](#), [8](#), [10](#), [20](#), [21](#), [26](#)
- [7] Hila Chefer, Yuval Alaluf, Yael Vinker, Lior Wolf, and Daniel Cohen-Or. Attend-and-excite: Attention-based semantic guidance for text-to-image diffusion models. *arXiv preprint arXiv:2301.13826*, 2023. [2](#), [3](#), [4](#), [6](#), [7](#), [8](#), [9](#), [10](#), [15](#), [17](#), [18](#), [20](#), [21](#)
- [8] Weixi Feng, Xuehai He, Tsu-Jui Fu, Varun Jampani, Arjun Akula, Pradyumna Narayana, Sugato Basu, Xin Eric Wang, and William Yang Wang. Training-free structured diffusion guidance for compositional text-to-image synthesis. *arXiv preprint arXiv:2212.05032*, 2022. [2](#), [3](#), [4](#), [7](#), [8](#), [10](#), [20](#), [26](#)
- [9] Jack Hessel, Ari Holtzman, Maxwell Forbes, Ronan Le Bras, and Yejin Choi. Clipscore: A reference-free evaluation metric for image captioning. *arXiv preprint arXiv:2104.08718*, 2021. [2](#), [3](#), [7](#)
- [10] Junnan Li, Dongxu Li, Caiming Xiong, and Steven Hoi. Blip: Bootstrapping language-image pre-training for unified vision-language understanding and generation. In *International Conference on Machine Learning*, pages 12888–12900. PMLR, 2022. [2](#), [3](#), [5](#), [7](#), [20](#), [26](#)
- [11] Junnan Li, Dongxu Li, Silvio Savarese, and Steven Hoi. Blip-2: Bootstrapping language-image pre-training with frozen image encoders and large language models. *arXiv preprint arXiv:2301.12597*, 2023. [2](#), [3](#), [7](#)
- [12] Roni Paiss, Hila Chefer, and Lior Wolf. No token left behind: Explainability-aided image classification and generation. In *Computer Vision—ECCV 2022: 17th European Conference, Tel Aviv, Israel, October 23–27, 2022, Proceedings, Part XII*, pages 334–350. Springer, 2022. [2](#)
- [13] Wonjae Kim, Bokyung Son, and Ildoo Kim. Vilt: Vision-and-language transformer without convolution or region supervision, 2021. [2](#)
- [14] Tao Xu, Pengchuan Zhang, Qiuyuan Huang, Han Zhang, Zhe Gan, Xiaolei Huang, and Xiaodong He. Attngan: Fine-grained text to image generation with attentional generative adversarial networks. In *Proceedings of the IEEE conference on computer vision and pattern recognition*, pages 1316–1324, 2018. [3](#)
- [15] Ming Tao, Hao Tang, Fei Wu, Xiao-Yuan Jing, Bing-Kun Bao, and Changsheng Xu. Df-gan: A simple and effective baseline for text-to-image synthesis. In *Proceedings of the IEEE/CVF Conference on Computer Vision and Pattern Recognition*, pages 16515–16525, 2022.
- [16] Hui Ye, Xiulong Yang, Martin Takac, Rajshekhar Sunderraman, and Shihao Ji. Improving text-to-image synthesis using contrastive learning. *arXiv preprint arXiv:2107.02423*, 2021.
- [17] Han Zhang, Jing Yu Koh, Jason Baldridge, Honglak Lee, and Yinfei Yang. Cross-modal contrastive learning for text-to-image generation. In *Proceedings of the IEEE/CVF conference on computer vision and pattern recognition*, pages 833–842, 2021.
- [18] Minfeng Zhu, Pingbo Pan, Wei Chen, and Yi Yang. Dm-gan: Dynamic memory generative adversarial networks for text-to-image synthesis. In *Proceedings of the IEEE/CVF conference on computer vision and pattern recognition*, pages 5802–5810, 2019. [3](#)

- [19] Aditya Ramesh, Mikhail Pavlov, Gabriel Goh, Scott Gray, Chelsea Voss, Alec Radford, Mark Chen, and Ilya Sutskever. Zero-shot text-to-image generation. In *International Conference on Machine Learning*, pages 8821–8831. PMLR, 2021. [3](#)
- [20] Yogesh Balaji, Seungjun Nah, Xun Huang, Arash Vahdat, Jiaming Song, Karsten Kreis, Miika Aittala, Timo Aila, Samuli Laine, Bryan Catanzaro, et al. ediffi: Text-to-image diffusion models with an ensemble of expert denoisers. *arXiv preprint arXiv:2211.01324*, 2022. [3](#)
- [21] Chenshuang Zhang, Chaoning Zhang, Mengchun Zhang, and In So Kweon. Text-to-image diffusion model in generative ai: A survey. *arXiv preprint arXiv:2303.07909*, 2023. [3](#)
- [22] Rosanne Liu, Dan Garrette, Chitwan Saharia, William Chan, Adam Roberts, Sharan Narang, Irina Blok, RJ Mical, Mohammad Norouzi, and Noah Constant. Character-aware models improve visual text rendering. *arXiv preprint arXiv:2212.10562*, 2022. [3](#)
- [23] Jonathan Ho and Tim Salimans. Classifier-free diffusion guidance. *arXiv preprint arXiv:2207.12598*, 2022. [3](#), [20](#)
- [24] Chenlin Meng, Yutong He, Yang Song, Jiaming Song, Jiajun Wu, Jun-Yan Zhu, and Stefano Ermon. SDEdit: Guided image synthesis and editing with stochastic differential equations. In *International Conference on Learning Representations*, 2022. [3](#)
- [25] Jooyoung Choi, Sungwon Kim, Yonghyun Jeong, Youngjune Gwon, and Sungroh Yoon. Ilvr: Conditioning method for denoising diffusion probabilistic models. *arXiv preprint arXiv:2108.02938*, 2021.
- [26] Jaskirat Singh, Stephen Gould, and Liang Zheng. High-fidelity guided image synthesis with latent diffusion models. *arXiv preprint arXiv:2211.17084*, 2022.
- [27] Omri Avrahami, Thomas Hayes, Oran Gafni, Sonal Gupta, Yaniv Taigman, Devi Parikh, Dani Lischinski, Ohad Fried, and Xi Yin. Spatext: Spatio-textual representation for controllable image generation. *arXiv preprint arXiv:2211.14305*, 2022.
- [28] Omer Bar-Tal, Lior Yariv, Yaron Lipman, and Tali Dekel. Multidiffusion: Fusing diffusion paths for controlled image generation. *arXiv preprint arXiv:2302.08113*, 2, 2023.
- [29] Vishnu Sarukkai, Linden Li, Arden Ma, Christopher Ré, and Kayvon Fatahalian. Collage diffusion. *arXiv preprint arXiv:2303.00262*, 2023.
- [30] Yu Zeng, Zhe Lin, Jianming Zhang, Qing Liu, John Collomosse, Jason Kuen, and Vishal M Patel. Scenecomposer: Any-level semantic image synthesis. *arXiv preprint arXiv:2211.11742*, 2022.
- [31] Zhengyuan Yang, Jianfeng Wang, Zhe Gan, Linjie Li, Kevin Lin, Chenfei Wu, Nan Duan, Zicheng Liu, Ce Liu, Michael Zeng, et al. Reco: Region-controlled text-to-image generation. *arXiv preprint arXiv:2211.15518*, 2022.
- [32] Lvmin Zhang and Maneesh Agrawala. Adding conditional control to text-to-image diffusion models. *arXiv preprint arXiv:2302.05543*, 2023.
- [33] Chong Mou, Xintao Wang, Liangbin Xie, Jian Zhang, Zhongang Qi, Ying Shan, and Xiaohu Qie. T2i-adapter: Learning adapters to dig out more controllable ability for text-to-image diffusion models. *arXiv preprint arXiv:2302.08453*, 2023.
- [34] Nataniel Ruiz, Yuanzhen Li, Varun Jampani, Yael Pritch, Michael Rubinstein, and Kfir Aberman. Dreambooth: Fine tuning text-to-image diffusion models for subject-driven generation. *arXiv preprint arXiv:2208.12242*, 2022.
- [35] Rinon Gal, Yuval Alaluf, Yuval Atzmon, Or Patashnik, Amit H Bermano, Gal Chechik, and Daniel Cohen-Or. An image is worth one word: Personalizing text-to-image generation using textual inversion. *arXiv preprint arXiv:2208.01618*, 2022. [3](#)
- [36] Alec Radford, Jong Wook Kim, Chris Hallacy, Aditya Ramesh, Gabriel Goh, Sandhini Agarwal, Girish Sastry, Amanda Askell, Pamela Mishkin, Jack Clark, et al. Learning transferable visual models from natural language supervision. In *International Conference on Machine Learning*, pages 8748–8763. PMLR, 2021. [3](#), [6](#), [18](#)
- [37] Jiahui Yu, Zirui Wang, Vijay Vasudevan, Legg Yeung, Mojtaba Seyedhosseini, and Yonghui Wu. Coca: Contrastive captioners are image-text foundation models. *arXiv preprint arXiv:2205.01917*, 2022.

- [38] Junnan Li, Ramprasaath Selvaraju, Akhilesh Gotmare, Shafiq Joty, Caiming Xiong, and Steven Chu Hong Hoi. Align before fuse: Vision and language representation learning with momentum distillation. *Advances in neural information processing systems*, 34:9694–9705, 2021. 3
- [39] Yushi Hu, Benlin Liu, Jungo Kasai, Yizhong Wang, Mari Ostendorf, Ranjay Krishna, and Noah A Smith. Tifa: Accurate and interpretable text-to-image faithfulness evaluation with question answering. *arXiv preprint arXiv:2303.11897*, 2023. 3
- [40] Kimin Lee, Hao Liu, Moonkyung Ryu, Olivia Watkins, Yuqing Du, Craig Boutilier, Pieter Abbeel, Mohammad Ghavamzadeh, and Shixiang Shane Gu. Aligning text-to-image models using human feedback. *arXiv preprint arXiv:2302.12192*, 2023. 4, 18, 19, 27
- [41] Xiaoshi Wu, Keqiang Sun, Feng Zhu, Rui Zhao, and Hongsheng Li. Better aligning text-to-image models with human preference, 2023. 4, 18, 19
- [42] Tom Brown, Benjamin Mann, Nick Ryder, Melanie Subbiah, Jared D Kaplan, Prafulla Dhariwal, Arvind Neelakantan, Pranav Shyam, Girish Sastry, Amanda Askell, et al. Language models are few-shot learners. *Advances in neural information processing systems*, 33:1877–1901, 2020. 5
- [43] Hugo Touvron, Thibaut Lavril, Gautier Izacard, Xavier Martinet, Marie-Anne Lachaux, Timothée Lacroix, Baptiste Rozière, Naman Goyal, Eric Hambro, Faisal Azhar, Aurelien Rodriguez, Armand Joulin, Edouard Grave, and Guillaume Lample. Llama: Open and efficient foundation language models. *arXiv preprint arXiv:2302.13971*, 2023. 5, 20, 24
- [44] Yiheng Liu, Tianle Han, Siyuan Ma, Jiayue Zhang, Yuanyuan Yang, Jiaming Tian, Hao He, Antong Li, Mengshen He, Zhengliang Liu, et al. Summary of chatgpt/gpt-4 research and perspective towards the future of large language models. *arXiv preprint arXiv:2304.01852*, 2023. 5, 20, 21, 24
- [45] AUTOMATIC1111. Stable-diffusion-webui. <https://github.com/AUTOMATIC1111/stable-diffusion-webui>, 2022. 6
- [46] Edward J Hu, Yelong Shen, Phillip Wallis, Zeyuan Allen-Zhu, Yuanzhi Li, Shean Wang, Lu Wang, and Weizhu Chen. Lora: Low-rank adaptation of large language models. *arXiv preprint arXiv:2106.09685*, 2021. 21
- [47] Rohan Taori, Ishaan Gulrajani, Tianyi Zhang, Yann Dubois, Xuechen Li, Carlos Guestrin, Percy Liang, and Tatsunori B. Hashimoto. Stanford alpaca: An instruction-following llama model. https://github.com/tatsu-lab/stanford_alpaca, 2023. 21
- [48] Christoph Schuhmann, Richard Vencu, Romain Beaumont, Robert Kaczmarczyk, Clayton Mullis, Aarush Katta, Theo Coombes, Jenia Jitsev, and Aran Komatsuzaki. Laion-400m: Open dataset of clip-filtered 400 million image-text pairs. *arXiv preprint arXiv:2111.02114*, 2021. 24
- [49] Christoph Schuhmann, Romain Beaumont, Richard Vencu, Cade Gordon, Ross Wightman, Mehdi Cherti, Theo Coombes, Aarush Katta, Clayton Mullis, Mitchell Wortsman, et al. Laion-5b: An open large-scale dataset for training next generation image-text models. *arXiv preprint arXiv:2210.08402*, 2022. 24

Divide, Evaluate, and Refine: Evaluating and Improving Text-to-Image Alignment with Iterative VQA Feedback

A Additional Results

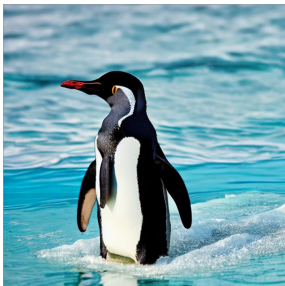
In this section, we include additional results for our approach which could not be included in the main paper due to space constraints. In particular, we report additional results for visualizing the iterative refinement process in Sec. A.1. We also provide additional results comparing our method performance with Attend-and-Excite [7] in Sec. A.2. Finally, in Sec. A.3, we compare our approach with recent contemporary work on using human feedback for improving text-to-image alignment.

A.1 Visualizing the Iterative Refinement Process

a man wearing a scuba suit playing a cello underwater with fish swimming around



a penguin wearing a bowtie standing on a surfboard in a swimming pool



a fish jumping out of the water to catch a butterfly near a waterfall

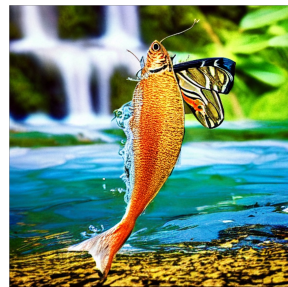
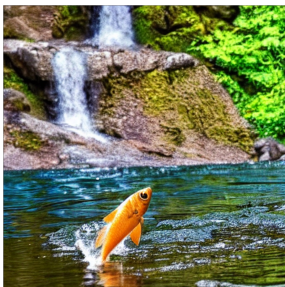


Figure 10: Visualizing iterative refinement process for improving text-to-image alignment.

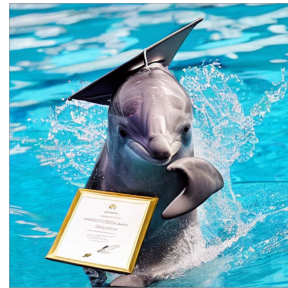
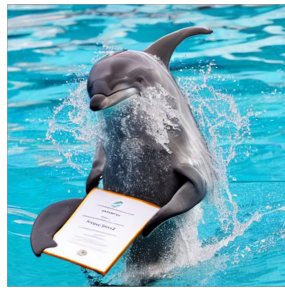
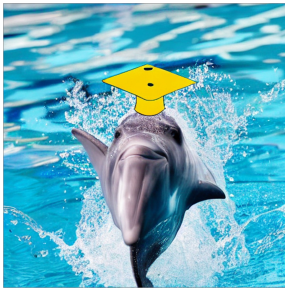
a cat wearing a life jacket on a canoe going down a river



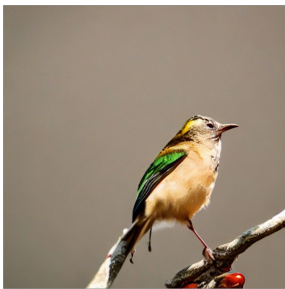
a monkey wearing a suit giving a presentation in a conference room



a dolphin wearing a graduation cap in a pool holding a diploma



a bird wearing a tiny hat on a branch next to a small cafe



a pod of dolphins jumping out of the water in an ocean with a ship in the background



Figure 11: Visualizing iterative refinement process for improving text-to-image alignment.

A.2 Additional Comparisons with Attend-and-Excite



Figure 12: *Additional Comparisons with Attend-and-Excite: Missing Relationship.* Due to the pure object focused nature of Attend-and-Excite [7], it may result in images where all objects are present but the relationship between them is not accurately described. In contrast, we observe that the iterative refinement approach is able to better describe both presence and relationship between the objects.



Figure 13: *Additional Comparisons with Attend-and-Excite: Overlapping Entities.* For images with overlapping entities (e.g., *person* and *spacesuit*), we observe that Attend-and-Excite [7] typically spends most of gradient updates balancing between the overlapping entities, as both entities (*person* and *spacesuit*) occupy the same cross-attention region. This can lead to outputs where a) other important aspects (e.g., *lake* in Col-3) or b) one of the two entities (e.g., *spacesuit*) are ignored.



Figure 14: *Additional Comparisons with Attend-and-Excite: Missing Objects.* Since Attend-and-Excite [7] is limited to applying the cross-attention update *w.r.t* the least dominant subject, as the complexity of input prompt increases, it may miss some objects (*e.g.*, umbrella, beach, sunny day) during the generation process. In contrast, the iterative nature of our approach allows it to keep refining the output image until a desirable threshold for the overall image-text alignment score is reached.

A.3 Comparisons with Human-Feedback based Methods

Besides training-free methods, recent contemporary work [40, 41] has also explored the possibility of improving image-text alignment using human feedback to finetune existing latent diffusion models. For instance, Wu *et al.* [41] recently release new versions of CLIP [36] and Stable Diffusion [1] models which have been finetuned to better align with user preferences using human-feedback data. In this section, we compare the performance of our simple training-free approach with models released by [41] in terms of both evaluation and improvement of fine-grain text-image matching.

Results. Fig. 15 compares the correlation of 1) Original CLIP [36] model, 2) HPS scores (CLIP model finetuned to better align with human preference scores) by [41], and 3) DA-Scores predicted by our method on the Decomposable-Captions-4k dataset. We observe that while the HPS scores with the finetuned CLIP model, show significantly higher correlation with human annotations as opposed to original CLIP model, it still performs worse than the proposed DA-scores.

Similarly, Fig. 16 compares the image outputs for 1) Original Stable Diffusion [1] model, 2) HPS Adapted Stable Diffusion model from [41] and 3) DA-score based iterative-refinement approach. We observe that while the HPS Adapted model improves the aesthetics of the generated model (*e.g.*, improved lighting in Col-1,5 in example-1 Fig. 16), it does not improve the semantic alignment with content of the input prompt. In contrast, while our approach does not improve the aesthetics of the generated image, the output images show significantly higher alignment with the input prompt.

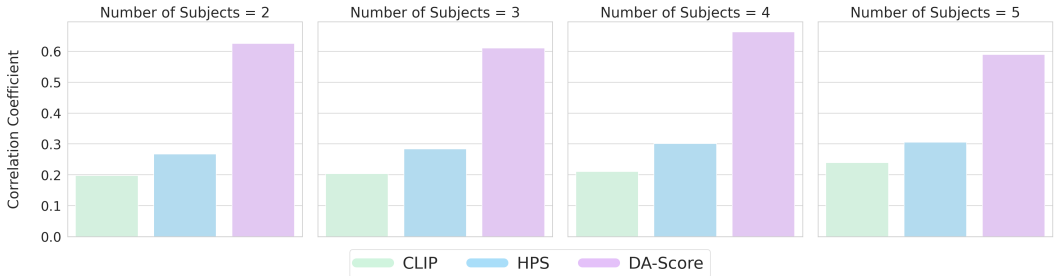


Figure 15: *Method comparisons w.r.t correlation with human ratings.* We compare the correlation of HPS score (CLIP finetuned with human feedback) from Wu *et al.* [41]. We observe that while the HPS score shows improved performance over CLIP [36], the proposed DA-score shows better correlation with human ratings across varying number of subjects in input prompt.

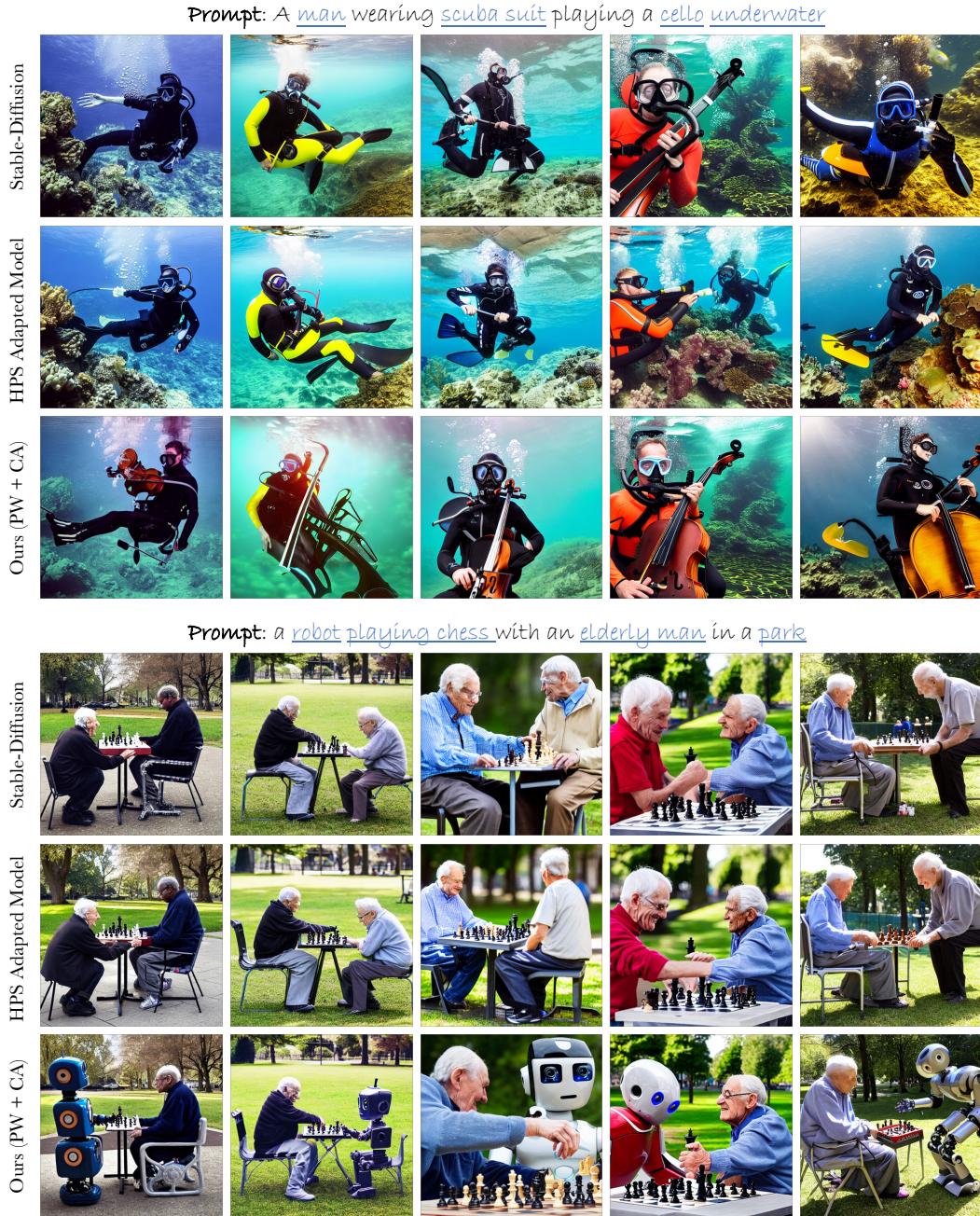


Figure 16: Comparing image alignment performance with human-feedback based models. We find that while human-feedback based finetuned diffusion model from [41] improves the aesthetics (e.g. lighting) of the output, it does not visually improve alignment with the input text for complex prompts.

Reason. As shown above while human preference finetuned CLIP and Stable Diffusion models from [41] show better performance in terms of aesthetics, they do not significantly improve visual alignment between generated images and input text as the complexity of the prompts increases. We believe that a major reason behind the same is the heavy data-driven nature of human-feedback based methods. That is, the generalization performance of the final finetuned model often relies heavily on the diversity and nature of the human-feedback dataset. In current works [40, 41], human-feedback is typically collected by showing users 4 – 10 images (for the same input prompt) generated by a pretrained Stable-Diffusion [1] model, and then asking the users to select the best match. However

	Prompt \mathcal{P} : A scuba diver <i>playing a guitar</i> underwater		
	Sub-prompts: $\{p_i\}$	Disjoint Assertion Set: $\{a_i\}$	Question Rephrasing: $\{a_i^q\}$
	a scuba diver. <u>playing a guitar</u> underwater	The image shows a scuba diver. The scuba diver is playing a guitar. The setting of scene is underwater.	Does the image show a scuba diver? Is scuba diver playing a guitar? Is setting of scene underwater?
	Prompt \mathcal{P} : A horse on a beach <i>wearing sunglasses</i>		
	Sub-prompts: $\{p_i\}$	Disjoint Assertion Set: $\{a_i\}$	Question Rephrasing: $\{a_i^q\}$
	a horse on a beach <u>wearing sunglasses</u>	The image shows a horse. The horse is on a beach. The horse is wearing sunglasses.	Does the image show a horse? Is the horse on a beach? Is the horse wearing sunglasses?
	Prompt \mathcal{P} : A dolphin <i>wearing a party hat</i> at a pool party		
	Sub-prompts: $\{p_i\}$	Disjoint Assertion Set: $\{a_i\}$	Question Rephrasing: $\{a_i^q\}$
	a dolphin <u>wearing a party hat</u> at a pool party	The image shows a dolphin. The dolphin is wearing a party hat. The setting of image is a pool party.	Does the image show a dolphin? Is dolphin wearing a party hat? Is setting of image pool party?

Figure 17: Visualizing the outputs of prompt decomposition. By dividing a complex prompt \mathcal{P} into a set of disjoint assertions a_i , we are able to identify the sub-prompts p_i (circled) which are not being expressed in the image output using VQA, and thereby address them using iterative refinement.

as shown in the main paper, as the complexity of the input prompt increases, the original Stable-Diffusion [1] model shows a very low text-to-image alignment accuracy. As a result, the collected human-feedback data is often biased towards predicting more aesthetically pleasing outputs, as opposed to outputs which improve fine-grain alignment with the content of the input prompt.

In contrast, we propose a simple training-free approach which is able to generalize well to both simple and hard prompts, for both evaluation and improvement of text-to-image alignment. We also note that training-free methods such as ours or prior works [6–8], can in-turn help improve the performance of human-feedback based methods by providing a better quality dataset for determining both aesthetics and content alignment of the generated images.

B Implementation Details

In this section, we provide further details for the implementation of our approach as well as other baselines [1, 6–8] used while reporting results in the main paper. The full detailed implementation for both evaluation and improvement of text-to-image alignment is provided in Alg. 1, 2.

Model Details. Similar to [7, 8], we use the official Stable Diffusion v1.4 model as the underlying pretrained text-to-image generation model while reporting results with all methods [6–8] (including the iterative refinement approach proposed in the main paper). All results are reported at 512×512 resolution while using 50 inference steps during the reverse diffusion process. Unless otherwise specified, a fixed classifier-free guidance scale [23] $\alpha_{cfg} = 7.5$ is used for all experiments. By default, we use the pretrained BLIP-VQA [10] model (BLIP model finetuned for visual question answering) for predicting the assertion-alignment scores while reporting all results.

Prompt Decomposition. Similar to our approach, prior works on improving image-text alignment often rely on human-user inputs for expressing contents of the input prompt into its simpler constituents. For instance, Feng *et al.* [6] require the user to describe the prompt as a conjunction / disjunction of simpler statements. Chefer *et al.* [7] require the user to provide a set of entities / subjects in the prompt, over which the cross-attention optimization should be performed. Similarly, in order to evaluate the *Decompositional Alignment Scores*, our approach relies on decomposing the input caption into a set of disjoint assertions (with their rephrasing as a question).

Instead of relying of human inputs as in prior works, we leverage the in-context learning capability of large-language models (LLMs) [43, 44] for obtaining such decompositions in an autonomous

manner. This allows us to perform large-scale quantitative evaluations across different methods in a robust manner. In particular, for all methods [6, 7] and ours, we first collect a set of 4-5 human generated examples describing the desired outputs (e.g., main subjects for [7]) for the input prompts. This example-set is then used as an in-context dataset which is then fed to the ‘gpt-4’ [44] model to generate the desired prompt decompositions on prompts across the *Decomposable-Captions-4k* dataset. Fig. 17 provides an overview of the different prompt decomposition outputs for our approach.

Note that while it is possible to explore relatively simpler methods e.g., extracting noun phrases for subject extraction in [7], it can lead to errors as the complexity of the input prompt increases. For instance, for the input prompt: “a *penguin* wearing a *bowtie* with a *bright sun* in the background”, the extracted noun phrases will also include the word “background”. The use of a LLM-based in-context framework allows us to avoid such errors. In future, the proposed approach can be extended to allow for much lightweight decomposition by using a low-rank finetuning [46] for adaptation of recently released instruction-following models [47]. However, since the same is not the main focus of our work, we leave it as a directive for future research.

Hyperparameters and Overall Algorithm. The proposed iterative refinement approach uses a maximum of $K = 5$ iterations for the refinement process. The iterative process is terminated early if a threshold of 0.8 for the overall image alignment score $\Omega(\mathcal{I}_k, \mathcal{P})$ is obtained. The iterative refinement weights are initialized as $w_i = 1 \forall i$ for prompt weighting (PW), and, $\gamma_i = 0 \forall i$ for cross-attention (CA) updates. An increment Δ of 0.1 and 1.0 is used for updating the assertion weights for prompt-weighting (PW) and cross-attention (CA) update methods respectively. Furthermore, to reduce the inference time for each iteration as compared to [7], cross-attention updates are only applied for first 20 steps of the reverse diffusion process. Furthermore, the use of iterative cross attention updates is also discarded. The image generation output \mathcal{I}^* at the end of the refinement process is computed as,

$$\mathcal{I}^* = \operatorname{argmax}_{\mathcal{I}_k} \Omega(\mathcal{I}_k, \mathcal{P}). \quad (7)$$

Please refer Alg. 1, 2 for the full detailed implementation (with hyperparameters) for our approach.

Algorithm 1 DA-Score: Evaluating Text-to-Image Alignment

Input: Text prompt \mathcal{P} , generated image \mathcal{I} .

Output: Text-to-Image Alignment Score between \mathcal{P}, \mathcal{I}

Require: Large-language model \mathcal{M} , VQA-model \mathcal{V} , exemplar dataset \mathcal{D} , task description \mathcal{T} , softmax-temperature $\tau = 0.9$

- 1: \triangleright **PROMPT DECOMPOSITION**
 - 2: $\mathbf{x} = \{x_0, x_1, \dots, x_n\} = \mathcal{M}(\mathbf{x} \mid \mathcal{P}, \mathcal{D}_{exemplar}, \mathcal{T})$, where $x_i = \{a_i, p_i, a_i^q\}$;
 - 3:
 - 4: \triangleright **COMPUTE ASSERTION ALIGNMENT SCORES USING VQA**
 - 5: $u_i(\mathcal{I}, a_i) = \frac{\exp(\alpha_i/\tau)}{\exp(\alpha_i/\tau) + \exp(\beta_i/\tau)}$, where $\alpha_i = \mathcal{V}(\text{‘yes’} \mid \mathcal{I}, a_i^q)$, $\beta_i = \mathcal{V}(\text{‘no’} \mid \mathcal{I}, a_i^q)$
 - 6:
 - 7: \triangleright **OVERALL IMAGE-TEXT ALIGNMENT SCORE**
 - 8: $\Omega(\mathcal{I}, \mathcal{P}) = \sum_i \lambda_i(\mathcal{P}, a_i) u_i(\mathcal{I}, a_i) / \sum_i \lambda_i(\mathcal{P}, a_i)$,
 - 9:
 - 10: **return** $\Omega(\mathcal{I}, \mathcal{P})$.
-

C Decomposable Captions 4K Dataset

Overview. Since there are no openly available datasets addressing semantic challenges in text-based image generation with human annotations, we introduce a new benchmark dataset Decomposable-Captions-4k for method comparison. The dataset consists an overall of 24960 human annotations on images generated using all methods [1, 6, 7] (including ours) across a diverse set of 4160 input prompts. Each image is a given rating between 1 and 5 (where 1 represents that ‘image is semantically irrelevant to the prompt’ and 5 represents that ‘image is an accurate match for the prompt’). Fig. 18 provides an overview of some user annotations for image-prompt pairs from the curated dataset.

Collecting Diverse Prompts of Varying Complexity. Furthermore, unlike prior works [7] which predominantly analyse the performance on relatively simple prompts with two subjects (e.g., object a and object b), we construct a systematically diverse pool of input prompts for better understanding

Algorithm 2 Iterative Refinement: Improving Text-to-Image Alignment

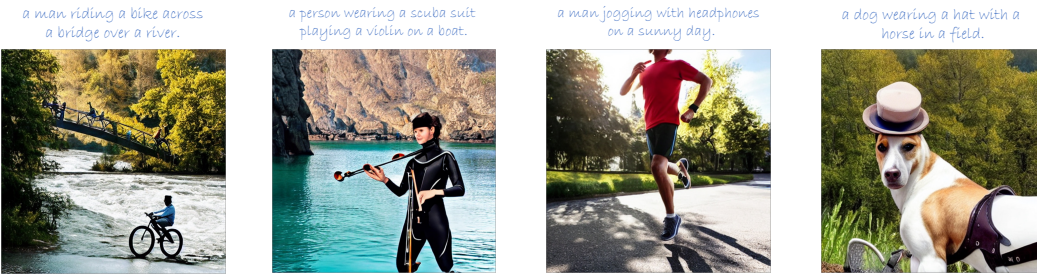
Input: Text prompt \mathcal{P} , subprompts p_i , disjoint assertions in question format a_i^q .
Output: Image generation output \mathcal{I}^* conditioned on \mathcal{P}
Require: Pretrained diffusion model \mathcal{D} , VQA-model \mathcal{V} , prompt-weighting function \mathcal{W}
Hyperparameters: max number of iterations $K = 5$, alignment threshold $\Omega_{max} = 0.8$, weight increments $\Delta_w = 0.1$, $\Delta_\gamma = 1.0$, step-size $\alpha = 10$, number of cross-attention update steps $t_0 = 20$.

- 1: \triangleright **INITIALIZE ASSERTION WEIGHTS**
- 2: Initialize $w_i^0 = 1 \forall i$; \triangleright for prompt-weighting
- 3: Initialize $\gamma_i^0 = 0 \forall i$; \triangleright for cross-attention updates
- 4:
- 5: \triangleright **ITERATIVE REFINEMENT**
- 6: **for** $0 \leq k < K$ **do**
- 7:
- 8: \triangleright **PROMPT WEIGHTING**
- 9: $y_{prompt} = \mathcal{W}(\mathcal{P}, \{\text{CLIP}(p_i), w_i^k\}_{i=1}^n)$;
- 10:
- 11: \triangleright **PARAMETERIZED REVERSE DIFFUSION**
- 12: Sample $z_T \sim \mathcal{N}(0, I)$;
- 13: **for** $0 < t \leq T$ **do**
- 14: $_, \mathcal{A}_i^t = \mathcal{D}(z_t, y_{prompt}, t)$; \triangleright compute cross-attention maps
- 15: **if** $t \geq T - t_0$ **then**
- 16: \triangleright **WEIGHTED CROSS-ATTENTION UPDATES**
- 17: $\mathcal{L}(z_t, \{\gamma_i^k\}_{i=1}^n) = \sum_i \gamma_i^k (1 - \max G(\mathcal{A}_i^t))$;
- 18: $z_t = z_t - \alpha \nabla_{z_t} \mathcal{L}(z_t, \{\gamma_i^k\}_{i=1}^n)$;
- 19: **end if**
- 20: $z_{t-1} = \text{REVERSEDIFF}(z_t, t \rightarrow t - 1 \mid y_{prompt})$;
- 21: **end for**
- 22:
- 23: \triangleright **GET DECOMPOSITIONAL-ALIGNMENT SCORES**
- 24: $\mathcal{I}_k = x_0 = \text{DECODER}(z_0)$;
- 25: $\Omega(\mathcal{I}_k, \mathcal{P}), \{u_i(\mathcal{I}_k, \mathcal{P})\}_i^n = \text{DA-SCORE}(\mathcal{I}_k, \{a_i^q\}_i)$;
- 26:
- 27: \triangleright **FINISH IF OUTPUT IS GOOD ENOUGH**
- 28: **if** $\Omega(\mathcal{I}_k, \mathcal{P}) \geq \Omega_{max}$ **then**
- 29: **return** $\mathcal{I}^* = \mathcal{I}_k$.
- 30: **end if**
- 31:
- 32: \triangleright **UPDATE ASSERTION WEIGHTS**
- 33: $w_i^{k+1} = \begin{cases} w_i^k + \Delta_w, & \text{if } i = \text{argmin}_l u_l(\mathcal{I}_k, \mathcal{P}) \\ w_i^k & \text{otherwise} \end{cases}$ \triangleright for prompt-weighting
- 34: $\gamma_i^{k+1} = \begin{cases} \gamma_i^k + \Delta_\gamma, & \text{if } i = \text{argmin}_l u_l(\mathcal{I}_k, \mathcal{P}) \\ \gamma_i^k & \text{otherwise} \end{cases}$ \triangleright for cross-attention updates
- 35: **end for**
- 36:
- 37: \triangleright **RETURN BEST OUTPUT**
- 38: **return** $\mathcal{I}^* = \text{argmax}_{\mathcal{I}_k} \Omega(\mathcal{I}_k, \mathcal{P})$.

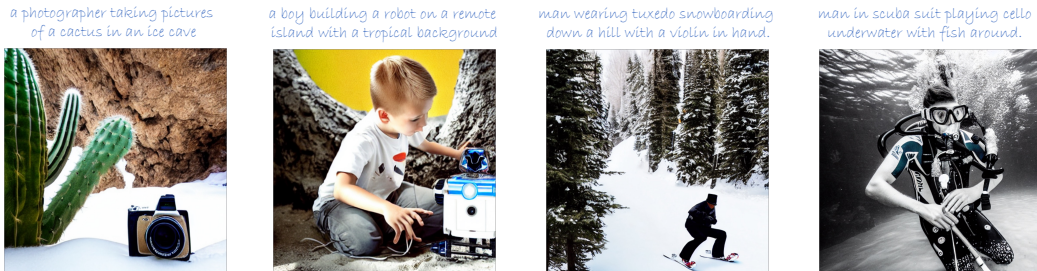
text-to-image alignment across varying complexities in the text prompt. In particular, the prompts for the dataset are designed to encapsulate two axis of complexity: *number of subjects* and *realism*. The number of subjects refers to the number of main objects described in the input prompt and varies from 2 (e.g., *a cat with a ball*) to 5 (e.g., *a woman walking her dog on a leash by the beach during sunset*). Similarly, the *realism* of a prompt is defined as the degree to which different concepts naturally co-occur together and varies as *easy*, *medium*, *hard* and *very hard*. *easy* typically refers to prompts where concepts are naturally co-occurring together (e.g., *a dog in a park*) while *very hard* refers to prompts where concept combination is very rare (e.g., *a dog playing a piano*).



(a) Example Samples with User Rating: 5 (Image is an accurate match for the prompt)



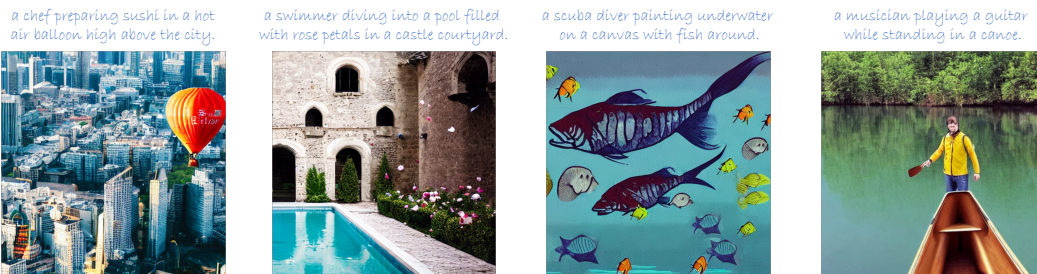
(b) Example Samples with User Rating: 4 (Image is a good match for prompt with minor mistakes)



(c) Example Samples with User Rating: 3 (Image seems like a 50-50 match for the prompt)



(d) Example Samples with User Rating: 2 (Image captures minor aspects about the input prompt)



(e) Example Samples with User Rating: 1 (Image seems semantically irrelevant to the prompt)

Figure 18: Visualizing samples with human annotations from the Decomposable-Captions-4k dataset.



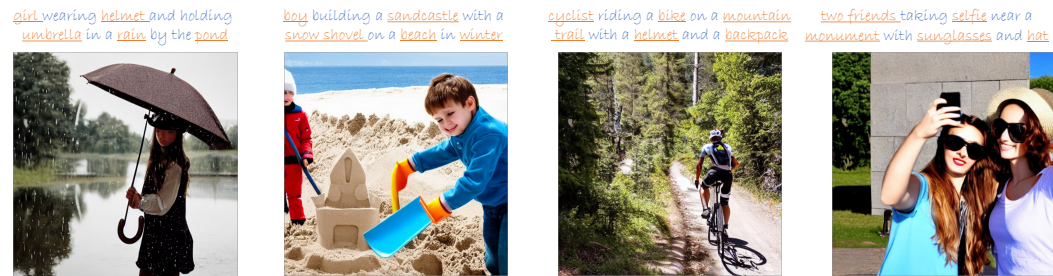
(a) Example sample outputs with our method for number of subjects: 2



(b) Example sample outputs with our method for number of subjects: 3



(c) Example sample outputs with our method for number of subjects: 4



(d) Example sample outputs with our method for number of subjects: 5

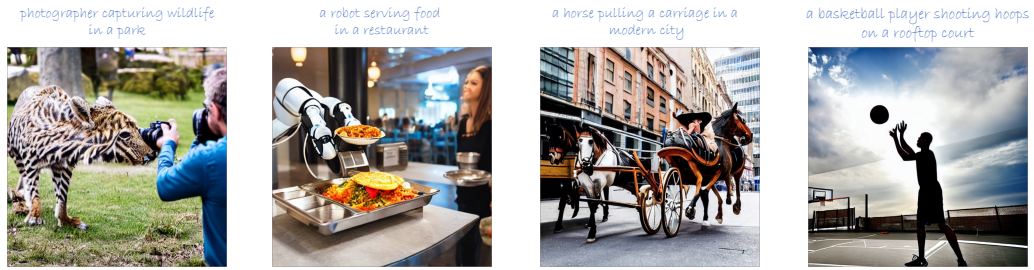
Figure 19: Visualizing variation in number of subjects in prompts from the Decomposable-Captions-4k dataset. All images are generated using the proposed iterative refinement approach.

Prompt Generation. A key part of the *Decomposable-Captions-4k* dataset is to collect a set of diverse input prompts of varying complexity which would allow for a much more comprehensive evaluation across different methods. Moreover unlike prompts found in typical large-scale image-text datasets [48, 49], the generated prompts should be imaginative and be able to describe novel and often non-realistic combinations of different concepts (e.g. a *lion playing a piano*).

To this end, we leverage the diverse language modelling capabilities of large-scale large language models (LLM) [43, 44] in order to generate novel prompts of varying complexity and realism. In particular, given a desired number of subjects N (between 2 and 5), we first use the *GPT-4* model [44] API with 8K context length to come up with an initial random subject e.g., a *dog*. The model is then instructed to conditionally generate a second subject (e.g., *sunglasses*) which is then combined with



(a) Example sample outputs with our method for realism difficulty: easy



(b) Example sample outputs with our method for realism difficulty: medium



(c) Example sample outputs with our method for realism difficulty: hard



(d) Example sample outputs with our method for realism difficulty: very hard

Figure 20: Visualizing variation in realism difficulty from the Decomposable-Captions-4k dataset. All prompts have been sampled using number of subjects = 3 subset of the overall dataset.

first subject to generate the sub-prompt “a *dog* wearing *sunglasses*”. This process is continued until a complete prompt with a desired number of subjects is obtained (e.g., a *dog* wearing *sunglasses* on a *skateboard* in a *park*). At the end of generation process, prompts which are grammatically inaccurate are filtered and removed. An overview of example prompts with variable number of subjects (along with corresponding image generation outputs with our approach) is provided in Fig. 19.

Furthermore, in order to generate prompts of varying level of *realism difficulty*, we generate prompts in batches of 4. In particular, during the sequential generation process (described above) the model is prompted to generate prompts of increasing level of *realism difficulty* by asking it generate additional subjects whose combination in a sentence is increasingly more rare. For instance, for *realism difficulty: easy*, the model is tasked to generate additional subjects which typically co-occur together



Figure 21: Setup for pairwise user study comparing our method with prior works.

in natural captions, which then leads to natural realistic prompts (e.g., *a group of friends having picnic under a tree*). As the *realism difficulty* is increased the model generates input prompts where the co-occurrence of different subjects is more and more rare, thus allowing it to generate more imaginative and challenging prompts (e.g. *a lion baking cookies in a kitchen*). Fig. 20 provides an overview of some example prompts with varying levels of realism difficulty.

Pairwise Human User Study. In addition to obtaining human annotations rating (between 1 to 5) for each image-prompt pair (refer Fig. 18), we also perform a pairwise user study comparing our method with prior works. In particular, given an input text prompt \mathcal{P} , the participants were shown a pair of image generation outputs comparing our method with prior works. For each pair, the human subject is then asked to select the output image which better aligns with the input prompt description. The human subjects are given three options *left*, *right* and *tie*, where *tie* indicates that both images are equally good or bad. All comparison images are generated using the same seed at 512×512 resolution with 50 inference steps for the reverse diffusion process. Fig. 21 provides a screenshot of the user interface for collecting the above human annotation data with pairwise comparisons.

D Discussion and Limitations

While the proposed iterative refinement approach shows better performance than previous works [6–8], it still has some limitations. *First*, the proposed decompositional approach relies on a pretrained BLIP-VQA model [10], for determining the alignment of the generated image with each of the disjoint assertions. Thus, weaknesses of the pretrained BLIP-VQA model become our weaknesses. Recall that the VQA scores help identify the areas in which the current image generation output is lacking, which can then be addressed in the next refinement step. However, if the VQA output is not correct, then the model might focus on assertions which are already well expressed, which can reduce the efficiency of the proposed iterative refinement strategy. In future, the use of more accurate VQA models e.g., BLIP2-VQA can help alleviate this problem. Furthermore, as noted through extensive quantitative experiments across a diverse range of input prompts (refer main paper and App. C), we find that the use of the BLIP-VQA model still yields quite competitive results.

Second, without additional information from the user, the iterative refinement approach considers all assertions to be equally important in determining the overall content of the input prompt. However, as

the complexity of the input prompt increases, we may wish to give more weight to certain parts of the prompt over the others. Furthermore, it is possible that the prompt may contain assertions which are not visually verifiable from the output image. For instance, for the prompt “*a penguin in a shopping mall on a weekend*”, the assertion about whether it is a weekend or not is not visually verifiable. Similarly certain actions *e.g.* searching, singing are also not verifiable from a single image. In future, we would like to explore a more autonomous mechanism for including additional information like 1) user ranking for different assertions (*i.e.*, what the user considers as important in a prompt) as well as 2) visual verifiability of a given assertion while computing the compositional alignment scores.

Finally, as noted in Fig. 7 of the main paper, we note that while the proposed iterative refinement approach leads to consistent improvements in alignment accuracy over prior works, the accuracy of the alignment process decreases as the complexity of input prompt is increased. In particular, for prompts with *very hard* realism difficulty, the overall alignment accuracy is only 62.9% (Attend-and-Excite has 49.5%). This leaves much room for improvement of text-to-image generation models. As discussed in App. A.3 one potential solution in this direction would be to combine recent works on human-feedback based diffusion model finetuning with the proposed training-free approach for data collection. In particular, by generating training data (on which human feedback is obtained) using the proposed iterative refinement strategy instead of previously used pretrained Stable Diffusion [1] models, we can increase the quality of the finetuning process. Using the proposed compositional alignment scores as pseudo-labels for learning the human-feedback based reward model [40] is another interesting direction for future work. However, the same is out of scope of this paper, and we leave it as a direction for future research.